

An algorithm to describe molecular scale rugged surfaces and its application to the study of a water/lipid bilayer interface

Sagar A. Pandit^{a)}

Department of Chemistry, University of North Carolina, Chapel Hill, North Carolina 27599

David Bostick^{b)}

Department of Physics and Program in Molecular/Cell Biophysics, University of North Carolina, Chapel Hill, North Carolina 27599

Max L. Berkowitz^{c)}

Department of Chemistry, University of North Carolina, Chapel Hill, North Carolina 27599

(Received 28 March 2003; accepted 24 April 2003)

We propose an algorithm for the general description of rugged molecular scale interfacial surfaces. This algorithm was implemented in the description of a phospholipid membrane/water interface with the rugged surface defined by the phospholipid phosphorous atoms. The method allowed us to clearly discern four layered regions of water based upon the water local density as a function of the distance from the membrane surface. Furthermore, the water in each of the layered regions was found to have distinct orientational properties. The classification we make based on density due to our new algorithm is in agreement with that delineated in previous studies based on water orientation. The contribution of the different water regions to the total electrostatic potential reveals the particular way in which each layer's water polarization contributes to the total dipole potential of the hydrated membrane. © 2003 American Institute of Physics. [DOI: 10.1063/1.1582833]

I. INTRODUCTION

The properties of macromolecules and molecular assemblies often hinge on the water in their surrounding environment. In particular, it is the water near an assembly's surface that plays a most crucial role. The characteristics of water near surfaces such as proteins, biomembranes, DNA, and micelles can be very different than those seen in bulk water. Thus, such interfacial water has been the subject of exhaustive experimental, simulation, and theoretical studies. Generally, water near the surface of such assemblies is placed into two categories: bound and free. Bound water is closer to the assembly's surface and has slower dynamical properties. Such water is typically called "slow" or "glassy,"¹⁻⁴ and in the specific case of biological systems the water is termed, "biological water."^{2,5,6} The free water is farther from the assembly's surface than the bound water, and is termed as such because of its bulklike properties.

The properties of bound and free water express themselves in very interesting ways in the cases of proteins and DNA molecules. Rocchi *et al.*⁷ and Makarov *et al.*⁸ have performed simulation studies that indicated that the translational and rotational diffusion of water is affected by the protein/water or DNA/water interface. Pal *et al.* characterized the interfacial water as bulk and rigidly bound water. They found that dynamics of water farther than 7 Å from the protein surface had essentially bulklike behavior.^{6,9} The molecular dynamics (MD) studies performed by Bizzarri and Cannistraro showed that water near the protein surface can be fur-

ther characterized by defining three classes: (i) strongly bound internal water; (ii) water interacting with the surface; and (iii) bulklike water. This characterization was based upon various static properties and the diffusion and orientational correlation times of water in each class.¹⁰ Similar dynamical properties of water are observed near the surface of surfactant micelles^{1-4,11} and for water in confined spaces.¹²⁻¹⁴

The discrepancy between the behaviors of free and bound water near the bilayer surface has been particularly well studied at the interface of phosphatidylcholine bilayer and water. It is known that water penetrates deeply into the surface of the L_α -phase bilayer at the bilayer/water interface.^{15,16} This penetration gives rise to a maximum hydration level for the L_α -phase of DPPC of 25 water molecules per lipid.¹⁷ It has been seen that some of the water in such a hydration level remains unfrozen at a temperature below 0 °C.¹⁸⁻²¹ Also, it is known that water at the interface has a diffusion coefficient almost 10 times smaller than bulk water.^{20,22}

There are many other properties of water near the surface of bilayers that contribute to their functionality. The water at the membrane/water interface is also highly polarized and shows a tendency to orient the water dipoles inwardly, such that the hydrogens are facing toward the center of the bilayer.²³ This interfacial water determines the sign and the value of the dipole potential,²⁴ which plays an important role in the passive permeation of ions across membranes.^{25,26} Interfacial water may affect the binding of peptides to the membrane surface.²⁷ In addition, the way in which interfacial water interacts with the membrane surface plays a critical role in the so called hydration force, thus

^{a)}Electronic mail: sagar@email.unc.edu

^{b)}Electronic mail: dbostick@physics.unc.edu

^{c)}Electronic mail: maxb@unc.edu

affecting the fusogenic properties of membranes.^{28,29} Thus, attention to the detailed nature of interfacial water properties near the bilayer surface, in particular, is warranted.

The aim of some simulation studies of water next to phospholipid bilayer has been to classify the water into regions near the bilayer.^{23,30} If one calculates the density profile of water next to a rather smooth wall, a layering profile due to the molecular packing effect is observed.³¹ Therefore, in this case, the assignment of water to different regions next to the interface can be easily accomplished. In the case of a phospholipid/water interface, a calculation of the water density profile as a function of the distance from the bilayer midplane produces a smooth profile due to the rough and broad character of the membrane surface. For this situation one may opt to classify water according to its orientational properties. Thus Jedlovsky and Mezei used the orientational ordering of water molecules as a criterion for their classification. Some of the classification methods used in simulation are analogous to those found in experimental studies. For example, Åman *et al.* used orientational order parameters derived from simulation data.³⁰ Similar order parameters are also measured in NMR experiments.³² Given that the difficulties in probing the interface are due to the rugged geometry of the bilayer surface, it may be interesting to investigate whether alternatives in the geometric constructs for the analysis of water properties near membranes can lead to a more detailed perspective for the characterization of interfacial water. We propose a novel algorithm for the analysis of the properties of a rugged interface. Application of this algorithm produces a water density plot that shows distinct regions of interfacial water. A similar algorithm was applied to the study of water structure at the water/micelle interface.¹ Also, coarser methods have been applied to study liquid/liquid interfaces.³³ In this work, our algorithm is specifically implemented for a rugged planar interface between phospholipid membrane and water. We have chosen to analyze the properties of the interfacial water in a MD simulation of a hydrated dipalmitoylphosphatidylcholine (DPPC) bilayer. (The structure of the DPPC molecule is shown in Fig. 1.)

II. MODEL AND METHODS

A. Simulation details

Molecular dynamics simulation was performed at the North Carolina Supercomputing Center using the GROMACS package.^{34,35} Force field parameters for lipids were based on the work of Berger.³⁶ The LINCS algorithm was used to constrain all bonds in the system³⁷ and allowed for a time step of 4 fs. Periodic boundary conditions were applied in all three dimensions. Long range electrostatics were handled using the SPME algorithm.³⁸ The temperature was maintained at 323 K using the Nosé–Hoover scheme with a thermostat relaxation time of 0.5 ps. The analysis of subsequent results was performed using a combination of GROMACS analysis utilities and our own code. The system was equilibrated in an NPT ensemble using the Parrinello–Rahman pressure coupling scheme^{39,40} with a barostat relaxation time of 2.0 ps at a pressure of 1 atm.

We performed a 10 ns simulation on a hydrated bilayer

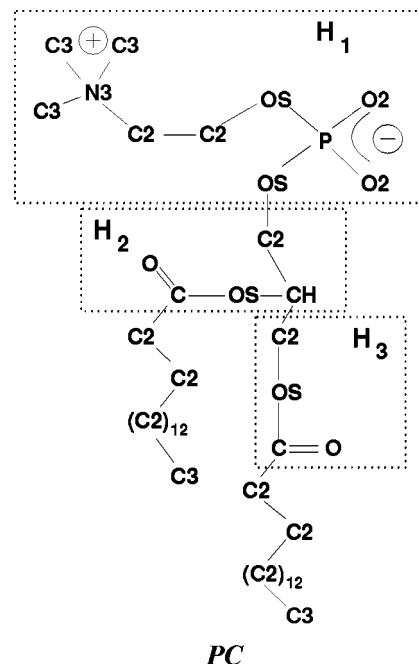


FIG. 1. The structure of a model DPPC molecule (Ref. 43). The regions H_1 , H_2 , and H_3 of the headgroup show three neutral groups.

consisting of 128 DPPC molecules and 6560 water molecules. An initial configuration for the system was taken from Tieleman.⁴¹ Sufficient equilibration was ensured by performing the analysis over the last 5 ns of the trajectory.

B. An algorithm to calculate the perpendicular distance from a rugged surface

The analysis of the properties of water parallel to the rugged membrane surface is done by essentially treating the surface as an assembly of “patches.” In order to quantify the distance of some species (in our case a water molecule) from this approximated surface, we introduce the quantity, d , obtained as follows in our system:

- (1) Since our system geometry is planar, we project the coordinates of the DPPC phosphorus atoms (or any other chosen DPPC atom) onto the plane $z=0$.
- (2) We perform a Voronoi tessellation⁴⁷ of the $z=0$ plane with the projected coordinates of the phosphorous atoms at the centers of the Voronoi polygons.
- (3) We then project the coordinates of the water molecules onto the $z=0$ plane.
- (4) A water molecule is associated with a Voronoi simplex if the projected coordinates of the water oxygen fall in the interior of that simplex.
- (5) The simplices are then lifted to the z -coordinates of their corresponding DPPC phosphorous atoms.
- (6) The distance from the surface of the bilayer, d , is now defined as the distance between the z coordinate of the water oxygen and the z coordinate of the corresponding lifted Voronoi simplex (see Fig. 2).

A schematic drawing depicting this analytical method is shown in Fig. 2.

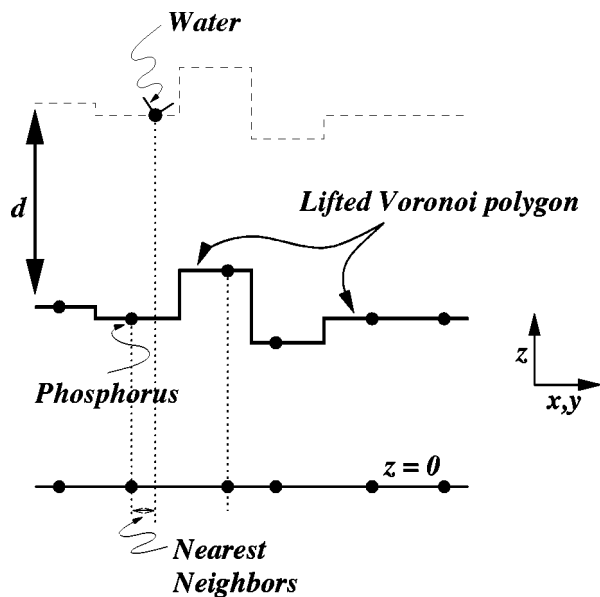


FIG. 2. Schematic diagram describing the algorithm for the calculation of the distance of a particle from a rugged surface.

III. RESULTS

A. Characterization of water

We calculate the density of water as a function of a distance d , from the surface defined by phosphorus atoms using the above described algorithm. The density profile can be thought of as a “surface-to-particle” correlation function. This density is shown in Fig. 3(a). Note that, unlike the z -density profile (z is a distance from the bilayer center), the water density in Fig. 3(a) is not a smooth sigmoidal function³⁰ as in Fig. 3(b). The density plot presented in Fig. 3(a) shows three regions of water. The first region is for distances below the point where the density plot displays a local minimum ($d \approx 0.4$ nm), the second region covers the range between the first density minimum and the point where the density achieves a bulk value (between $d \approx 0.4$ nm and $d \approx 1.0$ nm), and finally, the third region is for distances above $d \approx 1.0$ nm, where the density has a nearly constant bulklike value. In addition we observe that the density plot in the first region shows a hump around $d \approx -0.1$ nm and therefore we suspect that the density in this region is actually a superposition of two peaks. Another important functional group that is solvated by water and is close to the middle of the bilayer is the carbonyl group. Thus, we calculated the water density with respect to the surface defined by the carbonyl oxygens of the Sn-1 and Sn-2 chains. We also plot this density in Fig. 3(a). The two density plots shown in this figure allow us to separate water closer than 0.4 nm to the phosphate surface into two regions, and we refer to them as follows: region I is $1 \text{ nm} \leq d < -0.13 \text{ nm}$ (corresponding to water in the vicinity of carbonyl groups in the glycerol backbone), region II is $-0.13 \text{ nm} \leq d < 0.40 \text{ nm}$ (corresponding to water in the vicinity of the phosphocholine group), region III is $0.4 \text{ nm} \leq d < 1.00 \text{ nm}$ (corresponding to water in the second shell of the phosphocholine group), and region IV is $1.00 \text{ nm} \leq d$, where all the distances are from the approxi-

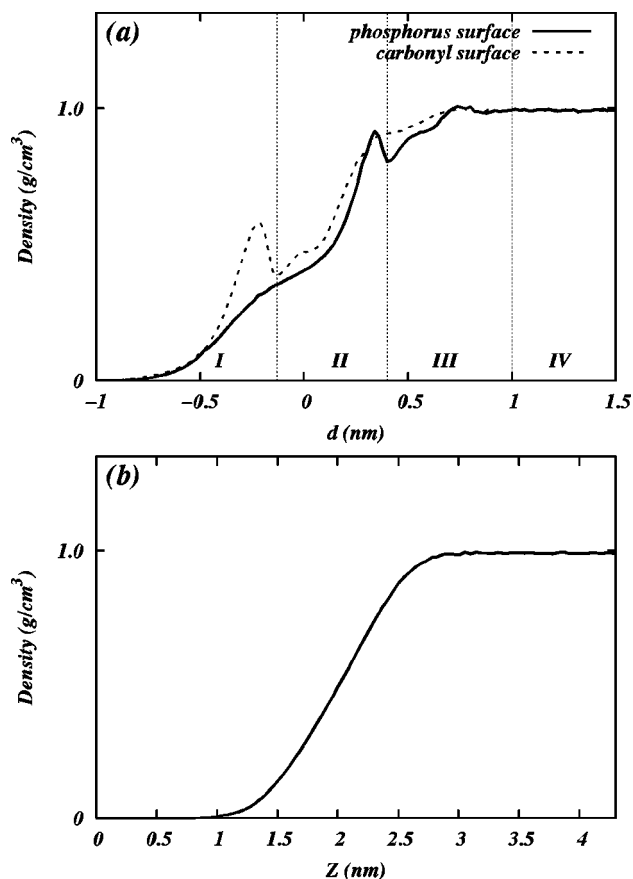


FIG. 3. (a) Surface-to-particle correlation function (density) for water with respect to the phosphorus and carbonyl surfaces. (b) surface-to-particle correlation function (z -density) for water with respect to an xy -plane placed at $z=0$.

imated surface made of phosphorus atoms in the DPPC head-group. Table I shows the variation of water density in each of the four regions.

Previous studies have shown that dynamical properties of water next to phospholipid surfaces are very different from properties of bulk water at the same temperature. It was observed that both translational diffusion and orientational correlation time are slowed down substantially.^{19,30} We calculated the translational and rotational motion characteristics for water in the regions determined from the density plot given in Fig. 3(a). The lateral diffusion coefficient of water is representative of its translational mobility in the xy -plane. It can be calculated from the long time behavior of the mean square displacement (MSD) of a water molecule using the Einstein relation,

TABLE I. The average density of water, ρ_{av} , lateral diffusion coefficient of water, D_{\parallel} , average number of water molecules per lipid, n_w , and the orientational correlation time, τ_1 of water for all four regions of water.

Regions	I	II	III	IV
ρ_{av} (g/cm ³)	0.069	0.553	0.918	0.986
$D_{\parallel} \times 10^{-9}$ (m ² /s)	0.583	1.464	3.528	4.772
n_w (No. of waters/lipid)	1.8	6.1	11.6	31.7
τ_1 (ps)	133.5	59.1	8.5	2.5

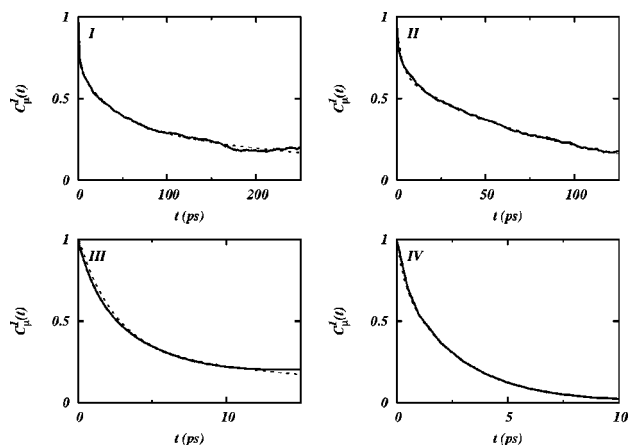


FIG. 4. First order orientational autocorrelation functions for water in regions I–IV.

$$D_{\parallel} = \lim_{t \rightarrow \infty} \frac{\langle |\boldsymbol{\rho}(t) - \boldsymbol{\rho}(t_0)|^2 \rangle}{4t},$$

where $\boldsymbol{\rho}$ is the lateral position of a water molecule in the xy -plane. We extracted this quantity from our trajectory as a function of the parameter d by dividing the d domain into 0.2 nm slabs. The MSD of each water molecule in each slab was calculated over 20 ps intervals in the 5 ns production run. Then, a least squares straight-line fit of the trajectory averaged MSD for each slab was performed over the subinterval from 5 to 18 ps within the 20 ps interval. The result for each region is reported in Table I. Diffusion of water is seen to be roughly 8 times smaller in region I than that in the bulk. This is consistent with observations made previously.²⁰ The value of the diffusion coefficient gradually increases in regions II and III until it reaches a bulk value in region IV (see Table I).

The orientational motion of water can be characterized by the dipolar autocorrelation function, $C_{\mu}^1(t) = \langle P_l(\boldsymbol{\mu}(0) \cdot \boldsymbol{\mu}(t)) \rangle$. The rotational correlation time, τ_1 can be calculated using the relation,

$$\tau_1 = \int_0^{\infty} dt C_{\mu}^1(t). \quad (1)$$

It was observed that the orientational autocorrelation function of “biological water” displays a slow component.^{1–6} To observe this slow component we need to perform our calculations with some care. If the autocorrelation function is calculated using all the water molecules located in their corresponding region at the beginning of the trajectory, molecules which cross regions during the trajectory would also be included in the calculation. Hence, we calculated the autocorrelation function for each region using only those water molecules that remained in their corresponding regions during the time period over which it was calculated. The functions were calculated up to 500, 250, 30, and 20 ps for regions I–IV, respectively. Figure 4 shows $C_{\mu}^1(t)$ for water in the four regions. From this figure we conclude that in regions I and II orientational motion of water contains a slow component that decays on a time scale of 100 ps, while the orientational decay of water in regions III and IV is an order of magnitude faster. To get more accurate

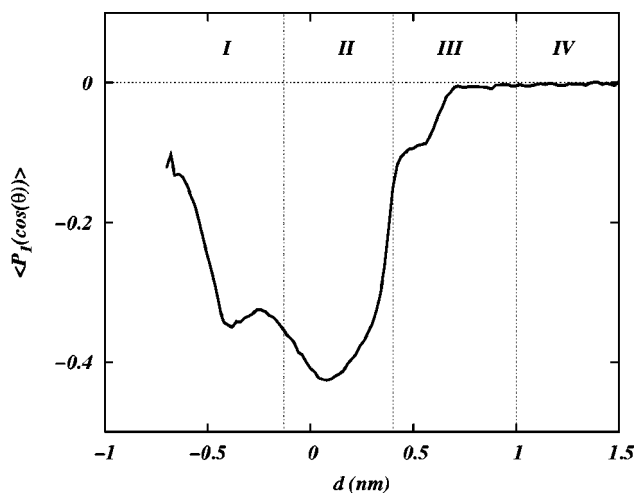


FIG. 5. First order dipolar order parameter for water as a function of d with respect to the surface of headgroup phosphorus atoms.

values for the rotational correlation time we fit each one of the correlation functions to a three-exponent function. These fitted functions were then used with Eq. (1) to obtain the water orientational correlation time for each region. These values are summarized in Table I. The correlation time in IV is in agreement with that found in bulk SPC water.⁴²

We assigned water in our system to regions I–IV using a local density plot [Fig. 3(a)]. According to the location of water molecules with respect to the bilayer we refer to water in regions I and II as being “bound” to the membrane. The water in region III can be characterized as “free” or “diffuse,” while that in IV is “bulklike.” The dynamical properties of water in these regions are consistent with this classification.

Studies which seek to classify water near the membrane/water interface usually use water orientational order parameters as a basis for classification criteria.^{23,30} Upon plotting the first dipolar order parameter as a function of d (Fig. 5), we can see a characteristic behavior of water in each region. The order parameter is either negative or zero in the entire domain of d indicating that water molecules in the interfacial region are orienting their dipoles inwardly. The minimum in region I at ~ -0.4 nm from the phosphorous surface is indicative of the strong inward orientation of water due to the carbonyl dipole of DPPC. The second minimum in II shows the strongest orientation. This suggests the orientational role of the large dipole formed by the phosphorous and nitrogen (P–N dipole) charges in the lipid headgroup. There is a small shoulder in III that implies a weak orientation. This is most likely also due to the influence of the P–N dipole. The behavior of the orientational profile in region IV, is similar to that in the bulk water. Correspondence between the shells in the density [Fig. 3(a)] and the shape of the first dipolar order parameter profile (Fig. 5) is evidence that our method of interfacial water classification is not inconsistent with the classification based on orientational properties of water.

Aman *et al.* identify “perturbed” interfacial water using the second orientational order parameter,³⁰ which is also measured by NMR experiment. In the simulation coordinate

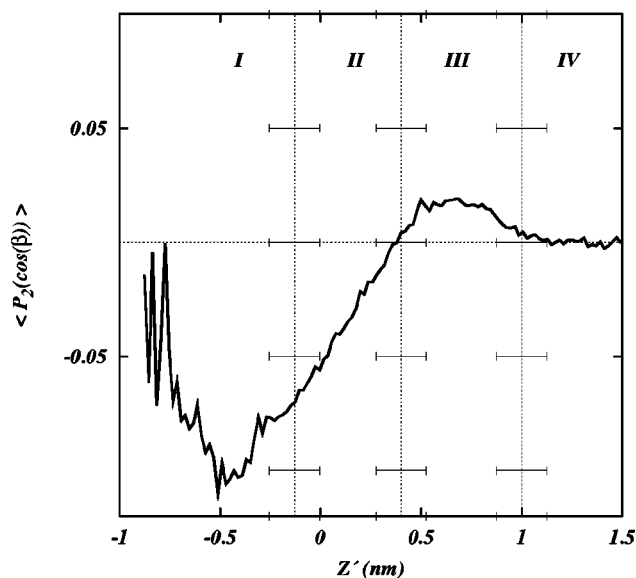


FIG. 6. Second order orientational order parameter for water as a function of Z' . The dotted lines define our four designated regions of water "blurred" by the width of the z -density of the DPPC phosphorus atoms.

system, the second orientational order parameter is $\langle P_2(\cos(\beta)) \rangle$, where β is the angle between the vector joining oxygen and either hydrogen of water and the z -axis. Specifically, they consider water to be perturbed if this order parameter is nonzero. This identification further classified the water into two regions based on the sign of the order parameter. A plot of this quantity has been provided in Fig. 6 (a similar plot is investigated by Aman *et al.*). The abscissa in this figure has been shifted so that the origin coincides with the peak of the z -density of the phosphorous atom. Hence we label the abscissa Z' rather than simply z . The function has clear negative (labeled B_- by Aman *et al.*) and positive (B_+) regions. Also, the order parameter is seen to be approximately zero as Z' reaches 1.2 nm in the bulklike region (labeled F). Since this figure's abscissa is not d , the vertical dotted lines defining our four water regions are blurred by the width of the z -density of the DPPC phosphorous atoms (illustrated by the horizontal error bars). It can be seen that the B_- region roughly corresponds to our regions I and II, the B_+ region roughly corresponds to our region III, and the F region roughly corresponds to our region IV. As further evidence of this correspondence in water classification, Aman *et al.* determined that the number of water molecules per lipid, n_w , in the B_- region is ~ 6 , while the sum of n_w in our regions I and II is ~ 8 (see Table I). Likewise, n_w in the B_+ region is ~ 11 , while in III it is ~ 12 . The total number of perturbed molecules per lipid in our case, $n_{w_{I+II+III}}$ is 19.5 while that determined by differential scanning calorimetry is at most 25.¹⁷ Note that the correlation between our classification and that of Aman *et al.* is solely based upon the calculation of the density as a function of the parameter d . Contrary to their method, no orientational information is used in defining our classification of interfacial water.

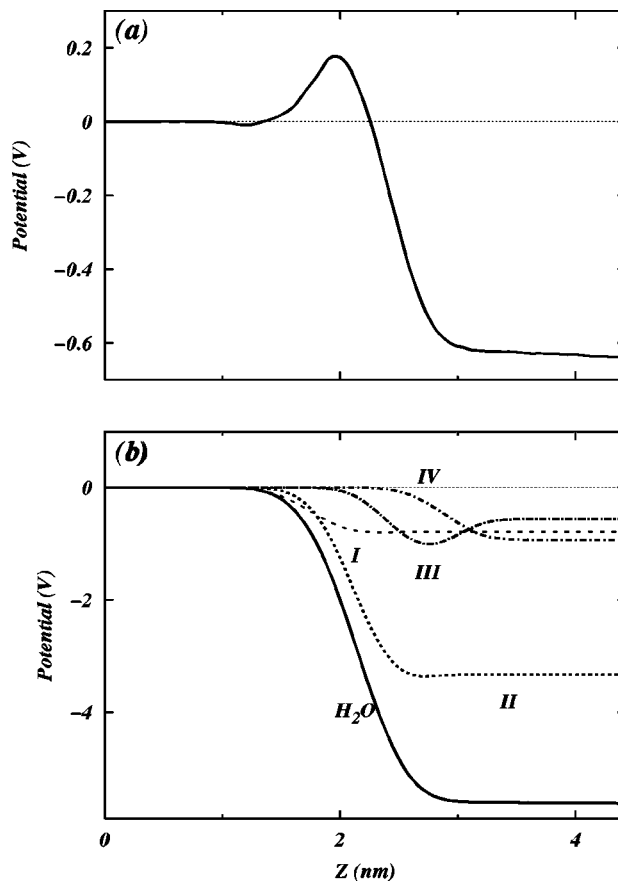


FIG. 7. (a) Dipole potential of the system as a function of z . (b) The contribution of each layer of water from regions I–IV to the total potential (solid line).

B. Electrostatics

The electrostatic potential obtained from simulation studies of lipid bilayers is normally calculated as a function of the bilayer normal (z) as follows:

$$\Phi(z) - \Phi(0) = -\frac{1}{\epsilon_0} \int_0^z dz' \int_0^{z'} \rho(z'') dz'', \quad (2)$$

where ρ is the local excess charge density in the system. We choose the zero of the potential at the center of the bilayer. The typical electrostatic potential profile for this type of system is negative in the bulk water with respect to the center of the bilayer. Simulation studies refer to the potential difference between these two regions as the "dipole potential"⁴³ in the case of neutral bilayers in pure water. Previous simulations using a similar force field obtain this potential difference to be approximately -600 mV.⁴³ We show in Fig. 7(a) the electrostatic potential profile of our system. It is in agreement with previous simulation studies.⁴³ Since the headgroup dipoles are arranged with their positive end oriented slightly outwardly, it is curious that a negative potential difference is observed. If water were treated as a dielectric continuum, one would expect this potential difference to be positive. Lin *et al.* emphasized that if the interfacial water is treated explicitly, this issue can be resolved.²⁴ They also attempted to

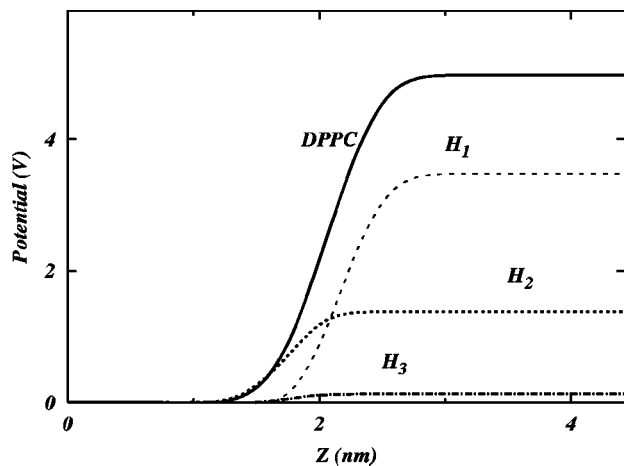


FIG. 8. The contribution of each region of the DPPC molecules defined in Fig. 1 to the total potential due to DPPC (solid line) as a function of z .

ascertain the extent to which water must be treated explicitly near the interface in order to obtain the appropriate electrostatic picture.

Using our algorithm, which assigns water to different regions, we can find out which of the four regions of water we describe is contributing the most to the electrostatic potential difference. The contribution of each region of water was obtained from the MD trajectory by assigning the system's water to the appropriate region based on its position along d for each snapshot. Equation (2) was then applied for each region in the snapshot. The total potential due to water and the average contribution to the potential of the water in each region is shown in Fig. 7(b). Note that region II contributes most significantly to the total potential due to water.

When speaking of the dipole potential, it is of interest to know which part of the lipid headgroup gives the greatest contribution. We break the headgroup into three major groups, each having a net neutral charge, and calculate the potential profile due to each group along with the total potential due to lipid in Fig. 8. Figure 1 shows the definition of each group. The group, H_1 is seen to give the largest contribution to the DPPC potential. The carbonyl groups, H_2 and H_3 , contribute the least. This is in agreement with conclusions obtained from experimental work.⁴⁴ Since the water in region II corresponds to the region occupied by the DPPC P–N dipole as detailed in our discussion of Fig. 5, it is clearly seen that both the P–N dipole from group H_1 and the water which orients due to the P–N dipole are the essential contributors to the dipole potential.

IV. SUMMARY

Solvent next to smooth molecular surfaces displays a layered density profile with respect to the surface. Therefore, it can be easily classified into regions depending on the distance from the surface. In the case of molecular scale rugged surfaces, the density profile with respect to some arbitrary plane parallel to the surface [in this case the xy -plane at $z = 0$ as in Fig. 3(b)] is smooth. Consequently, a more sophisticated procedure is required to resolve the molecular packing of solvent around that surface. Here, we propose an al-

gorithm that performs this task. When we applied our algorithm to a phospholipid/water interface, we were able to classify water into regions near this interface based on the evidence of water “shells” which pack closely near the membrane surface. It has been shown that distinct regions of water at the membrane/water interface can be outlined based solely upon a local density profile if that profile is depicted as a function of the parameter, d , the distance from the plane of phosphorous atoms formed by the lipid headgroups of the bilayer.

The regions of interfacial water as classified based on our algorithm are consistent with the classification obtained by other's calculations based upon water orientation.^{23,30} Furthermore, the number of water molecules per lipid in each of our regions is consistent with that obtained from the simulation of Aman *et al.* Since past studies' classification of water has been based upon water orientation, our classification method establishes a link between the water orientational properties of membrane bound water and the discrete nature of its packing near the membrane surface.

The classification we establish asserts that water in region II contributes the greatest amount to the total dipole potential. This is so because it most closely interacts with the P–N dipole of the DPPC headgroup. It is also observed that a negative dipole potential can be obtained only by explicitly treating the water in all four regions. Similar results have been obtained in the past.²⁴ Our classification is not resolved enough to say how large the layer of explicit water should be near the membrane surface before a continuum description will suffice in giving the correct sign and value of the dipole potential. This issue is well studied by Lin *et al.*²⁴

The utility of the method we describe for the description of a rugged surface is not limited to the analysis of water. Any molecular species can be described with respect to our surface description. For example, it will be useful to describe the distribution of ions in a salt solution with respect to a surface. Indeed, it has been shown that the rugged surface of membrane provides for very subtle issues in the depiction of ion binding.⁴⁵ Not only can one analyze the distribution of species other than water, but also, surfaces with a geometry other than planar can be described. For example one might use our algorithm for the description of the surface of a micelle. Water density has previously been calculated with respect to a micellar surface using this algorithm.¹ The finer details and implications of the algorithm have not been described, and are the focus of this work. Since, in essence, our method interpolates the surface under scrutiny using two-dimensional constant functions,⁴⁸ it can be used to describe any rugged surface with an underlying smooth geometry. Thus, the method we describe has implications for the study of many systems in which an interface plays an integral role.

Finally, we would like to mention that our classification of water is based on its distance from the surface defined by the positions of phosphorus atoms. We chose this surface because the peak-to-peak distance in the electron density obtained from x-ray measurements is used as a measure of the hydrophobic region of the membrane. The peak-to-peak distance is close to the average phosphorus–phosphorus distance. We also calculated the local density of water as a

function of the distance from a surface defined by nitrogen atoms and a surface defined by locations of the centers of masses of the headgroups. We did not observe serious differences upon taking these groups of atoms as surface-defining groups.

ACKNOWLEDGMENTS

This work was supported by the National Science Foundation under Grant No. MCB0077499 and also in part by the Molecular and Cellular Biophysics Program at the University of North Carolina at Chapel Hill under the USPHS training Grant No. T32 GM08570. Computational support from the North Carolina Supercomputing Center is gratefully acknowledged.

- ¹S. Senapati and M. L. Berkowitz, *J. Chem. Phys.* **118**, 1937 (2003).
- ²S. Pal, S. Balasubramanian, and B. Bagchi, *J. Chem. Phys.* **117**, 2852 (2002).
- ³S. Balasubramanian and B. Bagchi, *J. Phys. Chem. B* **105**, 12529 (2001).
- ⁴S. Balasubramanian and B. Bagchi, *J. Phys. Chem. B* **106**, 3668 (2002).
- ⁵N. Nandi and B. Bagchi, *J. Phys. Chem. B* **101**, 10954 (1997).
- ⁶S. K. Pal, J. Peon, B. Bagchi, and A. H. Zewail, *J. Phys. Chem. B* **106**, 12376 (2002).
- ⁷C. Rocchi, A. R. Bizzarri, and S. Cannistraro, *Phys. Rev. E* **57**, 3315 (1998).
- ⁸V. A. Makarov, M. Feig, B. K. Andrews, and B. M. Pettitt, *Biophys. J.* **75**, 150 (1998).
- ⁹S. K. Pal, J. Peon, and A. H. Zewail, *Proc. Natl. Acad. Sci. U.S.A.* **99**, 1763 (2002).
- ¹⁰A. R. Bizzarri and S. Cannistraro, *J. Phys. Chem. B* **106**, 6617 (2002).
- ¹¹S. Balasubramanian, S. Pal, and B. Bagchi, *Curr. Sci.* **82**, 845 (2002).
- ¹²N. E. Levinger, *Curr. Opin. Colloid Interface Sci.* **5**, 118 (2000).
- ¹³J. Faeder and B. M. Ladanyi, *J. Phys. Chem. B* **104**, 1033 (2000).
- ¹⁴J. Faeder and B. M. Ladanyi, *J. Phys. Chem. B* **105**, 11148 (2001).
- ¹⁵H. L. Casal and H. H. Mantsch, *Biochemistry* **26**, 4408 (1987).
- ¹⁶W. Hübner and A. Blume, *Chem. Phys. Lipids* **96**, 99 (1998).
- ¹⁷M. J. Ruocco and G. G. Shipley, *Biochim. Biophys. Acta* **691**, 309 (1982).
- ¹⁸C.-H. Hsieh and W.-g. Wu, *Chem. Phys. Lipids* **78**, 37 (1995).
- ¹⁹C.-H. Hsieh and W.-g. Wu, *Biophys. J.* **71**, 3278 (1996).
- ²⁰S. R. Wassall, *Biophys. J.* **71**, 2724 (1996).
- ²¹D. Chapman, R. M. Williams, and B. D. Ladbrooke, *Chem. Phys. Lipids* **1**, 445 (1967).
- ²²F. S. Volke, E. J. Galle, and G. Klose, *Chem. Phys. Lipids* **70**, 121 (1994).
- ²³P. Jedlovsky and M. Mezei, *J. Phys. Chem. B* **105**, 3614 (2001).
- ²⁴J.-H. Lin, N. A. Baker, and J. A. McCammon, *Biophys. J.* **83**, 1374 (2002).
- ²⁵S. B. Hladky and D. A. Haydon, *Biochim. Biophys. Acta* **318**, 464 (1973).
- ²⁶S. B. Hladky, *Biochim. Biophys. Acta* **352**, 71 (1974).
- ²⁷C. M. Shepherd, K. A. Schaus, H. J. Vogel, and A. H. Juffer, *Biophys. J.* **80**, 579 (2001).
- ²⁸J. Marra and J. Israelachvili, *Biochemistry* **24**, 4608 (1985).
- ²⁹G. Cevc, *J. Chem. Soc., Faraday Trans.* **87**, 2733 (1991).
- ³⁰K. Åman, E. Lindahl, O. Edholm, P. Håkansson, and P.-O. Westlund, *Biophys. J.* **84**, 102 (2003).
- ³¹C. Y. Lee, J. A. McCammon, and P. J. Rossky, *J. Chem. Phys.* **80**, 4448 (1984).
- ³²P.-O. Westlund, *J. Phys. Chem. B* **104**, 6059 (2000).
- ³³P. A. Fernandes, M. N. D. S. Cordiero, and J. A. N. F. Gomes, *J. Phys. Chem. B* **103**, 8930 (1999).
- ³⁴H. Berendsen, D. van der Spoel, and R. van Drunen, *Comput. Phys. Commun.* **91**, 43 (1995).
- ³⁵E. Lindahl, B. Hess, and D. van der Spoel, *J. Mol. Model.* [Electronic Publication] **7**, 306 (2001).
- ³⁶O. Berger, O. Edholm, and F. Jahnig, *Biophys. J.* **72**, 2002 (1997).
- ³⁷B. Hess, H. Bekker, H. J. C. Berendsen, and J. G. E. M. Fraaije, *J. Comput. Chem.* **18**, 1463 (1997).
- ³⁸U. Essmann, L. Perera, M. L. Berkowitz, T. Darden, H. Lee, and L. G. Pedersen, *J. Chem. Phys.* **103**, 8577 (1995).
- ³⁹S. Nose and M. L. Klein, *Mol. Phys.* **50**, 1055 (1983).
- ⁴⁰M. Parrinello and A. Rahman, *J. Appl. Phys.* **52**, 7182 (1981).
- ⁴¹D. P. Tieleman and H. J. C. Berendsen, *J. Chem. Phys.* **105**, 4871 (1996).
- ⁴²D. van der Spoel, P. J. van Maaren, and H. J. C. Berendsen, *J. Chem. Phys.* **108**, 10220 (1998).
- ⁴³A. M. Smondyrev and M. L. Berkowitz, *J. Comput. Chem.* **50**, 531 (1999).
- ⁴⁴K. Gawrisch, D. Ruston, J. Zimmerberg, R. P. Rand, and N. Fuller, *Biophys. J.* **61**, 1213 (1992).
- ⁴⁵S. A. Pandit, D. Bostick, and M. L. Berkowitz, *Biophys. J.* (to be published).
- ⁴⁶M. de Berg, O. Schwarzkopf, M. van Kreveld, and M. Overmars, *Computational Geometry: Algorithms and Applications*, 2nd rev. ed. (Springer-Verlag, Berlin, 2000).
- ⁴⁷The Voronoi tessellation of a set of points on a two-dimensional (2D) surface is a division of the surface into convex, space-filling polygons (called Voronoi simplices). Each polygon defines the region of the 2D-plane closest to each point in the set (see e.g. Ref. 46).
- ⁴⁸For example, in a spherically symmetric system one would use a spherical-polar coordinates. This implies that the constant functions interpolating the given surface will be arcs of a sphere.